Engineering Innovations
ISSN: 2813-1002, Vol. 18, pp 33-47
doi:10.4028/p-tO0BTR

Submitted: 2024-09-20
Revised: 2025-01-03
Accepted: 2025-01-07
Online: 2026-03-05

Impact of Satellite Orientation and Orbit Inclination on Thermal Transfers in a 1U LEO CubeSat

Ferdaous Tribak[1,a*], Othmane Bendaou[1,b], Fayçal Ben Nejma[2,c]

[1]OMS Research Team, Department of Physics, Faculty of Science, Abdelmalek Essaadi University, Tétouan, Morocco

[2]EMIR research laboratory, Monastir Preparatory Institute for Engineering Studies (IPEIM), University of Monastir, Monastir, Tunisia

[a*]ferdaous.tribak@etu.uae.ac.ma, [b]o.bendaou@uae.ac.ma, [c]faycal.bennejma@ipeim.rnu.tn

Keywords: heat transfer, CubeSat orientation, FEM, conduction, radiation, beta angle.

Abstract. The precision in temperature estimation plays a pivotal role in the design and operational efficiency of CubeSats. This study leverages the capabilities of COMSOL MULTIPHYSICS to model the thermal behavior of a 1U CubeSat, with a focus on evaluating the impact of orientation and beta angle on heat transfer dynamics and the resultant temperature distribution throughout the satellite. By conducting an extensive range of simulations that explore beta angles from 0° to 90° across four distinct satellite orientations, this research uncovers critical insights into the heat transfer mechanisms within the CubeSat framework. These findings illuminate the substantial influence of orientation and beta angle on the satellite's thermal state, highlighting the necessity of incorporating these factors into any comprehensive thermal analysis of spacecraft. The outcomes of this investigation not only contribute to a deeper understanding of CubeSat thermal management but also underscore the importance of meticulous design and analysis practices to optimize satellite performance in the challenging space environment.

Introduction

Before a satellite is launched, thorough analysis and testing are essential to anticipate and mitigate potential malfunctions and ensure efficient in-orbit performance. This is particularly vital for CubeSat projects, which adhere to the $10\times10\times10$ cm^3 dimensions of the standard 1U design. Most CubeSats in Low Earth Orbit (LEO) orbit below 600 km, with a quasi-circular orbit of around 100 minutes per period.

In LEO, Satellites are subject to internal heat and external space radiation including direct solar radiation, Earth's albedo, and infrared, resulting in extreme temperature variations critical to the operation of electrical components and mission success. Determining the temperature distribution in orbit enables the selection of thermal control equipment and the avoidance of high temperature gradients. The main aim of thermal control is therefore to study satellite temperatures, design control mechanisms and test the proposed solutions [1,2].

Given the importance of understanding how nanosatellites respond to such thermal environments, various numerical methods have been developed to predict temperature variations in space. For example, Reyes et al. [03] created a MATLAB algorithm based on the Finite Difference Method (FDM) for thermal simulations and compared its results with those obtained from the commercial Thermal Desktop software. Similarly, Bulut and Sozbir [04] conducted a numerical study to examine the temperature distribution of nanosatellites at different altitudes and with varying panel configurations. Another study by Bonnici et al. [05] focused on the PocketQube UoMBSat-1, employing a thermal model based on the Lumped Parameter Method (LPM) and comparing the results to those generated by commercial software like Ansys®. Their findings confirmed that passive thermal control is effective when using appropriate software tools based on the Finite Element Method (FEM).

In addition to numerical modeling, passive thermal control strategies have also been investigated extensively. Corpino et al. [06] demonstrated that passive thermal coatings can effectively maintain nanosatellite components within their operational temperature ranges, considering both internal and external heat generation. Moreover, researchers at Chosun University's STEP Cube Lab in Korea [07] evaluated the performance of a multi-layer insulation (MLI) system, made of glass and Kapton, which enabled thermal-passive designs that maintained acceptable temperature levels throughout the mission.

Further advances in the field have been achieved by comparing different modeling approaches. Kovács and Józsa [08], for instance, performed a comparative analysis between thermal network models and finite element models, highlighting their application to the thermal design of small satellites. Moffitt's work [09] on the Combat Sentinel satellite incorporated multilayer insulation to predict temperatures under extreme orbital heating conditions. Other efforts, such as those by Morsch Filho et al. [10], used the commercial ANSYS software, which employs the Finite Volume Method (FVM), to simulate the thermal performance of a 1U CubeSat in both cold and hot worst-case scenarios.

Karthigesu Thanarasi [11] contributed to the field by performing thermal analysis in extreme hot and cold environments using the Finite Element Analysis (FEA) method with MSC Software's Nastran and Patran packages. Tsai [12], on the other hand, developed a general thermal mathematical model incorporating conductive and radiative heat transfer, with environmental heating and cooling treated as boundary conditions. In parallel, Reiss [13] used a MATLAB-based software tool to enhance the precision of nanosatellite thermal modeling, comparing the results to those obtained with professional tools like ESATAN-TMS.

The novelty of this study lies in its unprecedented integration of beta angle and orientation analysis within a single framework, offering a comprehensive understanding of CubeSat thermal behavior under varying orbital conditions. Unlike previous works that analyze these factors independently, our research leverages advanced simulation techniques to uncover their combined impact. This integrated approach not only fills a critical gap in existing literature but also provides actionable insights for improving satellite performance and reliability in Low Earth Orbit.

Orbit Environment Heating Fluxes

The temperature of the CubeSat results from the fluxes it encounters in orbit. It is therefore a function of orbital parameters (altitude, inclination, beta angle representing the angle between the solar vector and the orbit plane, etc.), satellite geometry, materials and surface properties.

In order to determine the temperature of the CubeSat, the heat balance must be implemented to take into account all the energy entering and leaving the system. The overall transient energy balance of the Cubesat is as follows [14, 15].

$$Q_{Solar} + Q_{Albedo} + Q_{IR} + Q_{Gen} - Q_{Rad} = m \cdot C_{avr} \cdot (dT_{avr}/dt). \quad (1)$$

With:

- Q_{Solar} : Heat input from direct solar radiation [W].
- Q_{Albedo} : Heat input from reflected solar radiation [W].
- Q_{IR} : Heat input from Earth's infrared emission [W].
- Q_{Gen} : Internally generated heat within the satellite [W].
- Q_{Rad} : Heat lost by the satellite due to radiation [W].
- M : Mass of the satellite [kg].
- C_{avr} : Average specific heat capacity of the satellite [J/kg·K].
- dT_{avr}/dt : Rate of change of the satellite's average temperature, [K/s].
- t = Time [s].

Where:

$$Q_{solar} = \alpha_s . A_{prj} .S. \quad (2)$$

$$Q_{albedo} = \alpha_s .A_{prj} .S. a .F_{sat\text{-}planet}. \quad (3)$$

$$Q_{IR} = \alpha_{IR} .A_{prj} .Q_E.F_{sat\text{-}planet}. \quad (4)$$

$$Q_{rad} = \varepsilon .\sigma.T^4. A_{tot} . \quad (5)$$

With:

- α_S: solar absorptivity of the surface [-].
- α_{IR}: infrared radiation absorptivity of the earth [-].
- ε: Emissivity of infrared radiation [-].
- S : Solar constant [W/m²].
- Q_E: Infrared energy emitted by the Earth [W/m²].
- a : Albedo factor.
- $F_{sat\text{-}planet}$: Form factor between the surface of the CubeSat and the Earth.
- σ: Stefan-Boltzmann constant [W/(m^2 K^4)].
- A_{prj}: Surface area of CubeSat exposed to radiation [m^2].
- A_{tot}: Total surface area of CubeSat [m^2].
- T: CubeSat temperature [°C].
- T_{avr}: Average satellite temperature [°C].
- C: Average specific heat.
- m: Satellite mass.

The figure below illustrates the heat exchange dynamics between the satellite and its surrounding space environment.

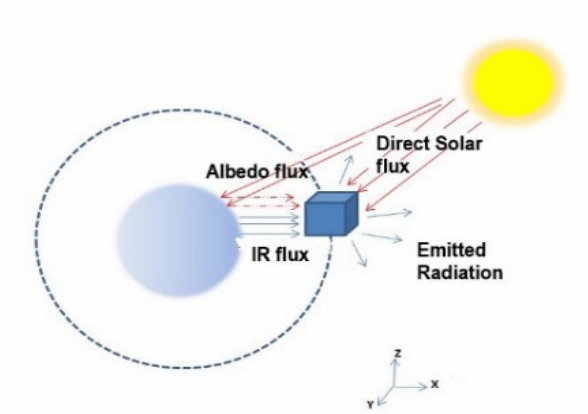

Fig. 1. Heat exchange between the satellite and the space environment.

CubeSat Thermal Analysis

Beta Angle

An influential parameter in this analysis is the beta angle, which determines the amount of time the CubeSat is exposed to direct sunlight. Beta angle is also described as the angle between the plane of orbit and the solar vector of any object orbiting the Earth. The beta angle varies between +90° and -90°, depending on the direction of the satellite. [16,17,18]

Changes in the beta angle result in different orientations of the orbit plane in to the Sun and the Earth, leading to different temperature ranges.

The following figure shows the definition of the beta angle [18].

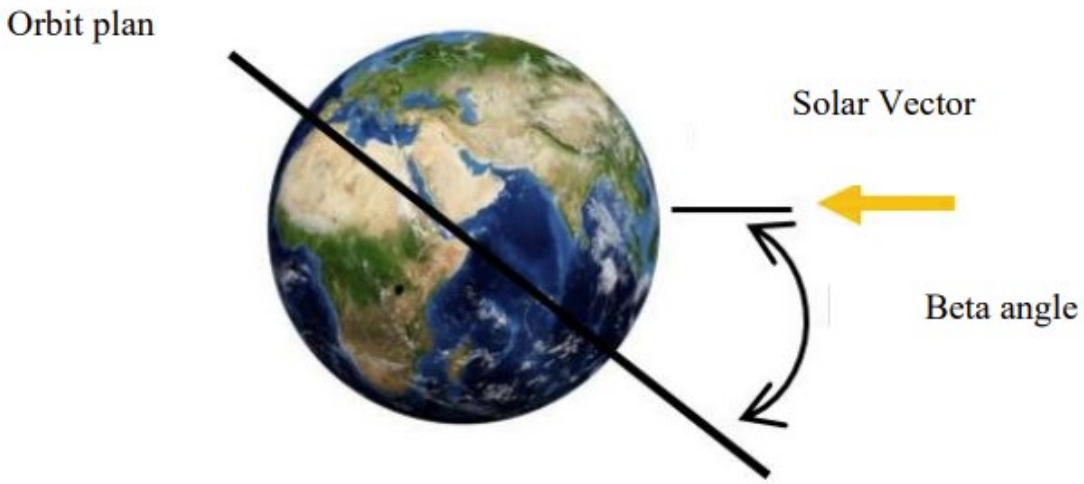

Fig. 2. Beta angle definition.

Satellite Orientation

The second main parameter taken into account in this analysis is the orientation of the satellite. The orientation direction of the CubeSat is very important to the thermal an altitude control engineers. They often seek to increase aerodynamic drag by placing large deployable elements, such as solar panels, so as to obtain a maximum surface area normal to the spacecraft velocity vector. For this reason, it is common to make compromises in spacecraft altitude and configuration to reduce the thermal impact of the aerobraking maneuver. Deployable elements, which often have a low thermal mass per unit area, require particular attention in the thermal analysis to ensure that temperature requirements are not exceeded. Similarly, if the orientation vector of the spacecraft has a known uncertainty, the thermal engineer needs to explore several possible orientation angles to ensure that the most critical airbrake for each sensitive component is identified [14].

COMSOL Multiphysics Simulation

In this study, COMSOL Multiphysics was chosen for its advanced Multiphysics capabilities, which enable accurate modeling of coupled thermal phenomena, and its ability to handle the complex boundary conditions encountered in satellite thermal analysis. Its intuitive interface, combined with efficient solvers, makes it a reliable and widely recognized tool for thermal simulations in aerospace applications.

Geometry

The geometry represents a hollow cube 10 cm x 10cm x 10 cm. Its six faces represent the solar panels with a thickness of 2 mm.
All the details related to the internal structure, wiring, connectors and electronics have not been included in this work because the interest is on a more generic simulation of a 1U CubeSat.

Meshing

The meshing was done by the integrated mesher. The size of the elements has been set to fine. The complete mesh consists of 42365 elements. With a minimum quality equal to 0.2228, and an average quality equal to 0.6665.

Material Properties

Only one material is considered for the simplified structure of the satellite, the table below shows its physical properties.

Table 1. Material properties.

Density (ϱ)	2810 [kg/m^3]
Specific heat (Cp)	948 [J/kg K]
Thermal conductivity (K)	140 [W/mK]

Satellite Orientation

In this study, a detailed thermal analysis is conducted for each of the four orientations showcased below.

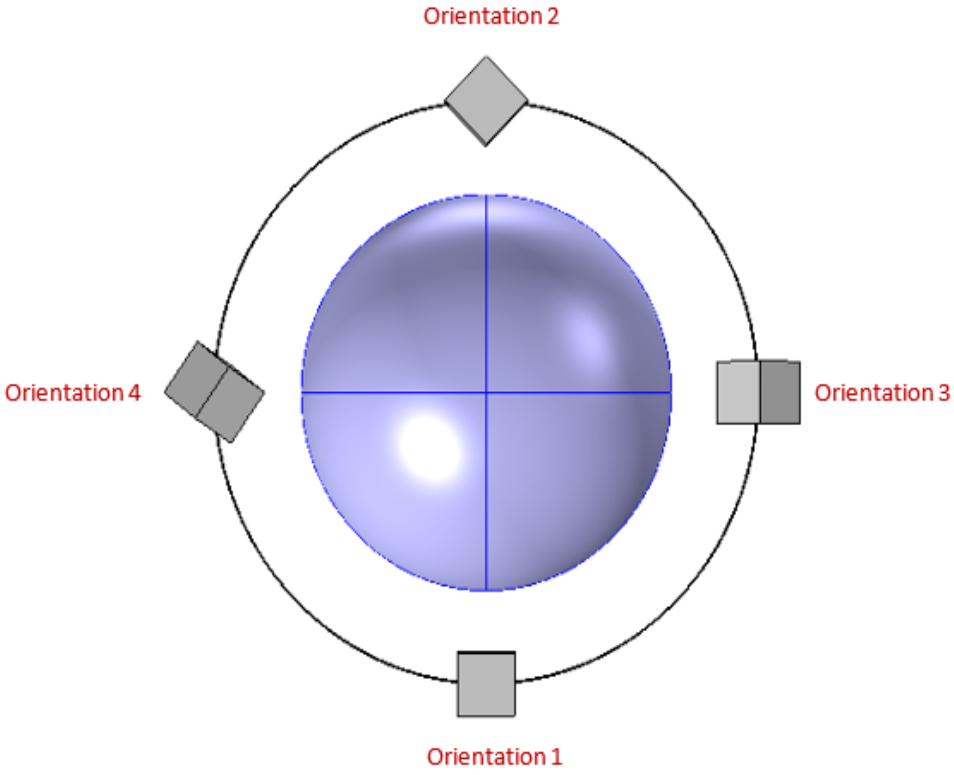

Fig. 3. The four studied orientations of the satellite in LEO.

Altitude and Orbit

The satellite describes a circular orbit, at an altitude of 431 km, which corresponds to a period of 5583 s.

View Factors

Direct solar radiation is a function of the inclination of a given face to the Sun, which is presented as a point source, but IR radiation and albedo will come from a spherical source close to the satellite, and the incident radiation is not known in advance. In this case, an appropriate view factor must be taken into account. This parameter actually quantifies the amount of radiation emitted by body 1 that is collected on the surface of body 2 [19,20].

Several expressions are provided in the literature, but those of interest to us in this study relate to plates receiving energy from a spherical source, in the representation of faces parallel or perpendicular to the Earth's surface [1,20].

The view factors of the various surfaces at the altitude already indicated and for the four orientations are shown in the table below.

Table 2. View factors values.

Orientation	$F_{1\rightarrow earth}$	$F_{2\rightarrow earth}$	$F_{3\rightarrow earth}$	$F_{4\rightarrow earth}$	$F_{5\rightarrow earth}$
1	0.876	0.281	0.281	0.281	0.281
2	0.652	0.033	0.652	0.033	0.281
3	0.652	0.033	0.281	0.281	0.033
4	0.574	0.067	0.574	0.067	0.574

Boundary Conditions

The thermal boundary conditions for this study were designed to replicate the typical environment experienced by a CubeSat in Low Earth Orbit (LEO). To summarize the key points discussed in the preceding sections, the table below provides a concise overview of the boundary conditions and assumptions underlying this COMSOL simulation. This summary aims to clearly outline the foundational parameters and simplifications that define the scope and methodology of the analysis.

Table 3. Boundary conditions.

Direct solar radiation	1367 [W/m^2]
Earth IR emission	240 [W/m^2]
Earth's reflected solar radiation (albedo)	410 [W/m^2]
Albedo coefficient	0.3 [-]
Solar absorptivity (α_s)	0.87 [-]
IR absorptivity (α_{IR})	0.8 [-]
IR Emissivity (ε)	0.81 [-]
Altitude	431 [km]
Period	5583 [s]
Beta angle	[0°, 90°]

Results and Discussion

The studied satellite has been analyzed in different beta angles (0°, 10°, 20°, 30°, 40°, 50°, 60°, 70°, 80°, 90°) in order to evaluate its impact on heat transfer and satellite temperature.
The simulation is done on 5 periods to reach the stationary regime, in 27900 s.
Below are the simulation results for the beta angle equal to 0.

Orientation 1

The CubeSat is oriented so that the (X+) side of the cube is facing the sun, and the (X-) side is facing the earth.
Below in Figure 4, the simulation outcomes for a beta angle of 0° are presented.

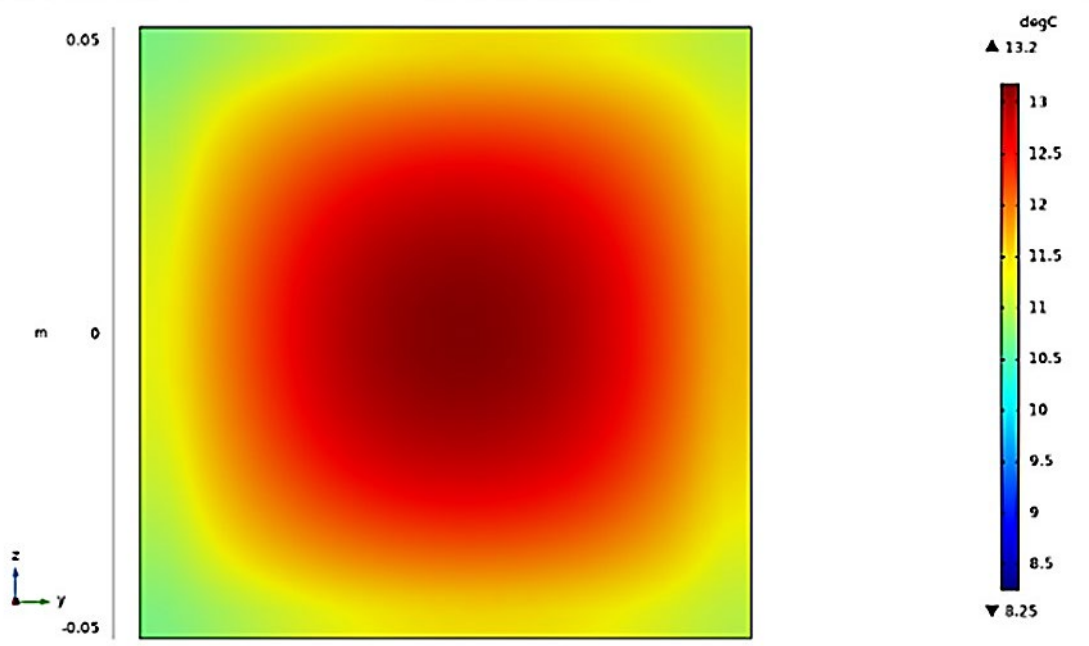

Fig. 4. Temperature variation of the satellite for β =0° at time 27900 s - view of orientation 1 on the (YZ) plane on COMSOL Multiphysics.

Due to the low thermal conduction of the solar panel, a significant temperature gradient develops across its surface. This phenomenon results in a pronounced temperature peak at the center, while the edges exhibit minimum values. The disparity arises because heat transfer is limited, leading to uneven thermal distribution across the panel.

The curves depicted in Figure 5 illustrate the variations in temperature (°C) across the satellite's surfaces over time (s).

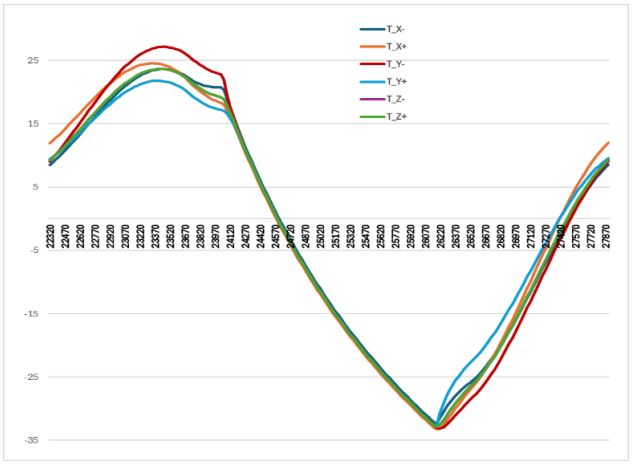

Fig. 5. Variation of the temperatures of the satellite's faces as a function of time.

Face (X+) receive more radiation at the beginning of the orbit resulting in maximum temperature for this side in that instant as shown in Figure 5. However, the maximum overall temperature is achieved by side (Y-) because it's already warmer when the solar radiation starts to raise its temperature. In comparison, side (Y+) has similar incoming radiation to side (Y-), but it's colder than side (Y-) when the solar flux heats it. Side (X+) stays warmer than other sides near the end of the eclipse because it receives radiation from the earth due to its projection toward that source. The minimum occurs on solar panel (X-) because it does not receive any radiation from the sun or the earth during the eclipse. Sides (Z+) and (Z-) have the same thermal behavior because their projection toward the radiation sources are identical.These two surfaces do not have significative variation because they do not receive solar radiation, only Abedo emission from the earth, and for this reason only one curve appears in the plot.

Orientation 2

The Z axis of orientation 1 is rotated of -45°. This new direction defines the orientation 2. The figure below depicts the temperature fluctuations of the satellite when it is aligned with Orientation 2, with the beta angle set at β = 0°.

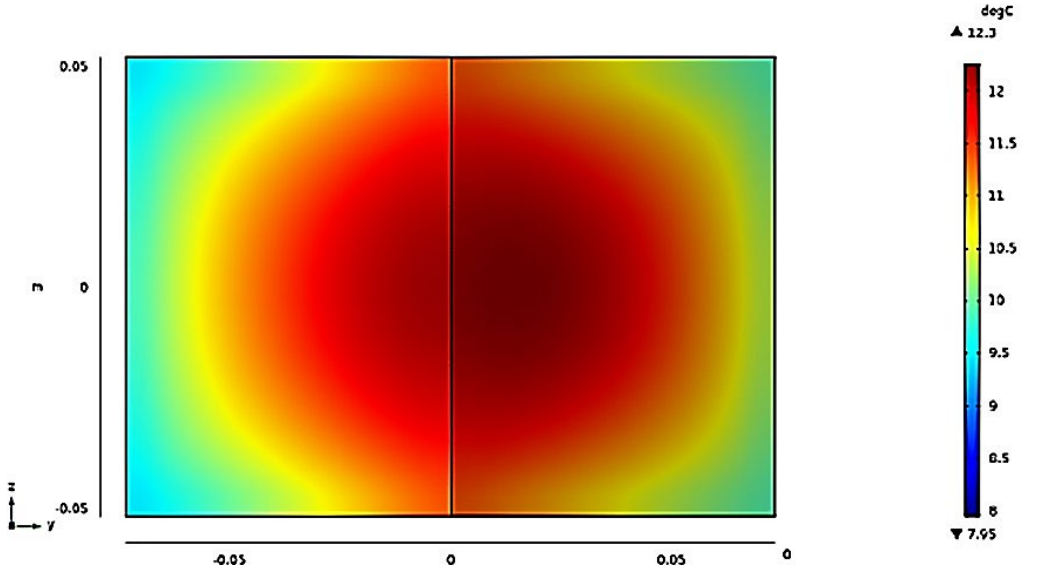

Fig. 6. Temperature variation of the satellite for β =0° at time 27900 s - view of orientation 2 on the (YZ) plane on COMSOL Multiphysics.

The peak of temperature at the intersection of the (X+) and (Y+) faces is due to the orientation of the surfaces towards the sun during the period of sunshine, this part of the satellite receives the greatest amount of direct solar radiation.
Figure 7 features curves that display the changing temperatures across the surfaces of the satellite as time progresses.

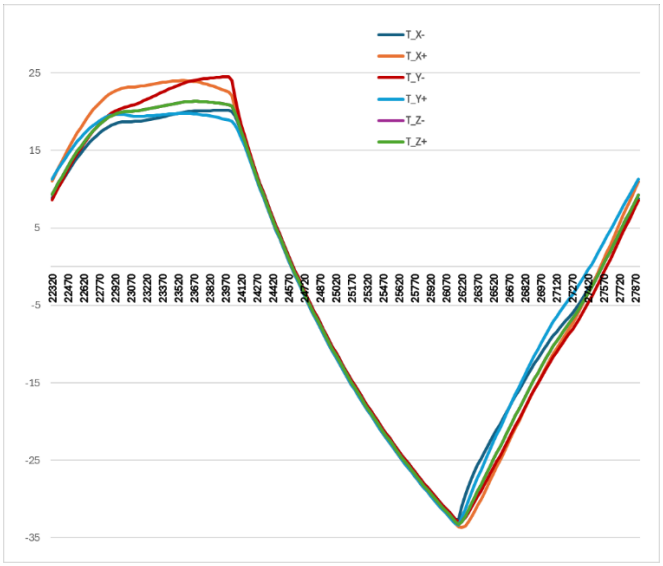

Fig. 7. Variation of the temperatures of the satellite's faces as a function of time.

Due to this specific orientation, both the (Z-) and (Z+) sides receive equal amounts of incoming radiation. Consequently, only five plots are depicted on the graph.

Orientation 3

The Y axis of orientation 1 is rotated of -45°. This new direction defines the orientation 3.
The figure below demonstrates the temperature distribution across the satellite at β = 0°, when it is aligned with Orientation 3.

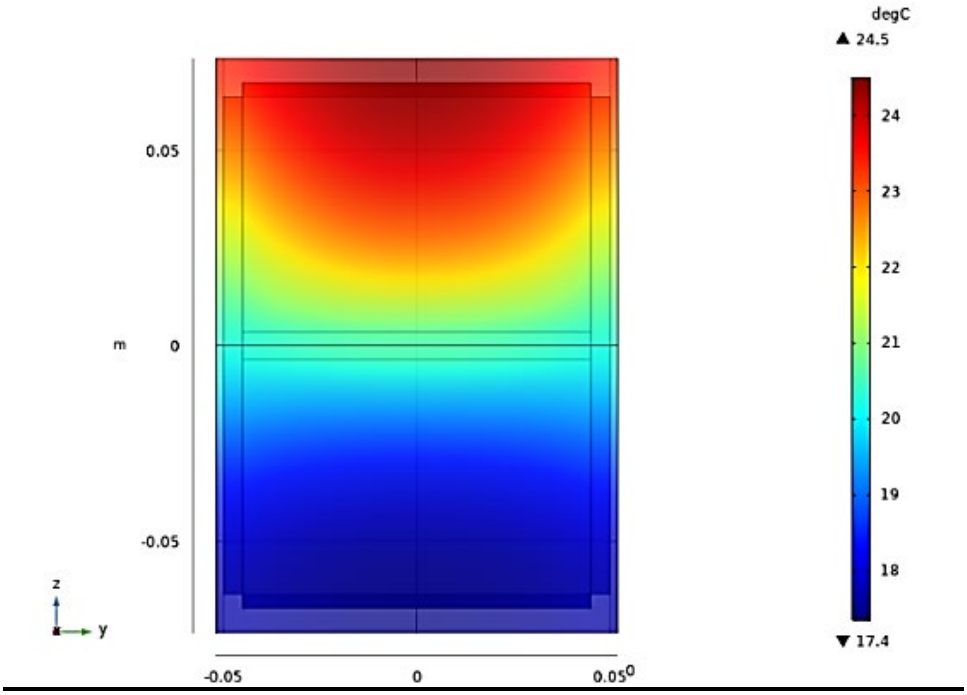

Fig. 8. Temperature variation of the satellite for β =0° at time 27900 s - view of orientation 3 on the (YZ) plane on COMSOL Multiphysics.

Figure 9 presents curves illustrating the dynamic changes in temperature across the satellite's surfaces over time, specifically when the satellite is set to Orientation 3.

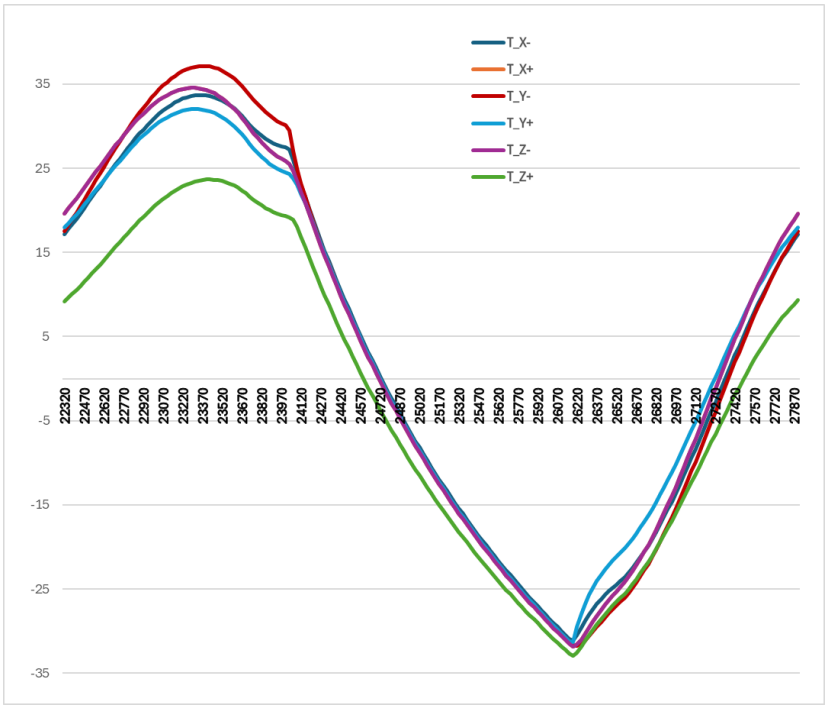

Fig. 9. Variation of the temperatures of the satellite's faces as a function of time.

Due to this specific orientation, the (X-) and (Z+) surfaces receive the same amount of incoming radiation, as do the (X+) and (Z-) surfaces. Consequently, the graph only displays four plots to represent these matching radiation levels.

Orientation 4

In Orientation 1, the Z-axis undergoes a rotation of -45 degrees. Subsequently, the Y-axis is rotated by arctan(1/√2)*180/π degrees to align the cube's diagonal towards the Earth. This adjustment establishes Orientation 4.
The figure presented below offers a view of the temperature distribution throughout the satellite when it is aligned in Orientation 4, with the beta angle (β) set at 0°.

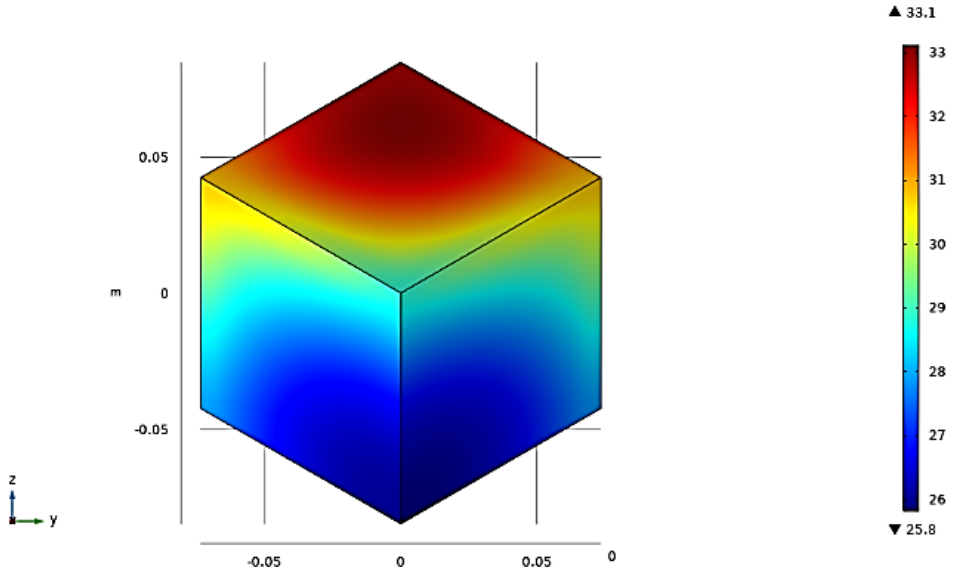

Fig. 10. Temperature variation of the satellite for β =0° at time 27900 s - view of orientation 4 on the (YZ) plane on COMSOL Multiphysics.

Figure 11 showcases graphs depicting the temporal variations in temperature across different surfaces of the satellite, particularly when it is oriented in Position 3.

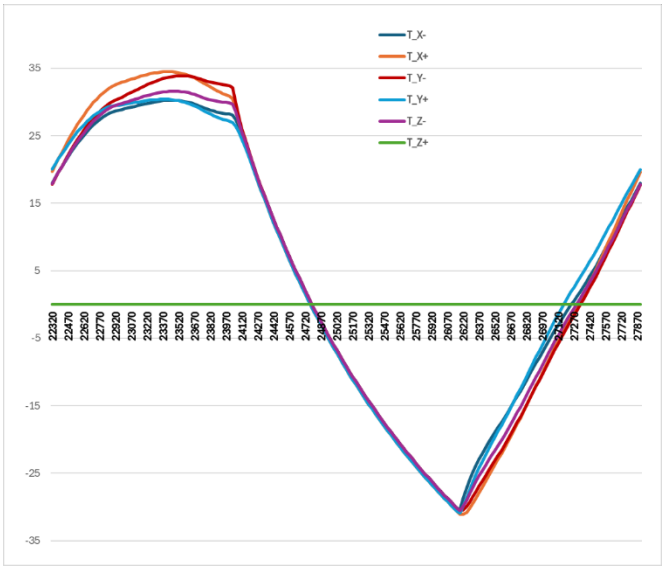

Fig. 11. Variation of the temperatures of the satellite's faces as a function of time.

To underscore the significance of the beta angle, also known as orbit inclination, a series of simulations were conducted across a range of beta angles from 0 degrees to 90 degrees. This was done to evaluate the influence of orbit inclination on heat transfer dynamics and the extreme temperatures experienced by the satellite.

Figures 12, 13, 14, and 15 present charts that display the minimum and maximum temperatures experienced by the satellite across various beta angles and orientations. These charts are essential for illustrating how the satellite's temperature fluctuates with its positioning relative to Earth and the Sun. They highlight the impact of the satellite's orientation and beta angle on temperature changes, with each figure representing a different orientation and its influence on heat exposure. This analysis plays a crucial role in emphasizing the significance of orientation and beta angle in the satellite's temperature management, aiding in the design and operational strategies for maintaining optimal thermal conditions.

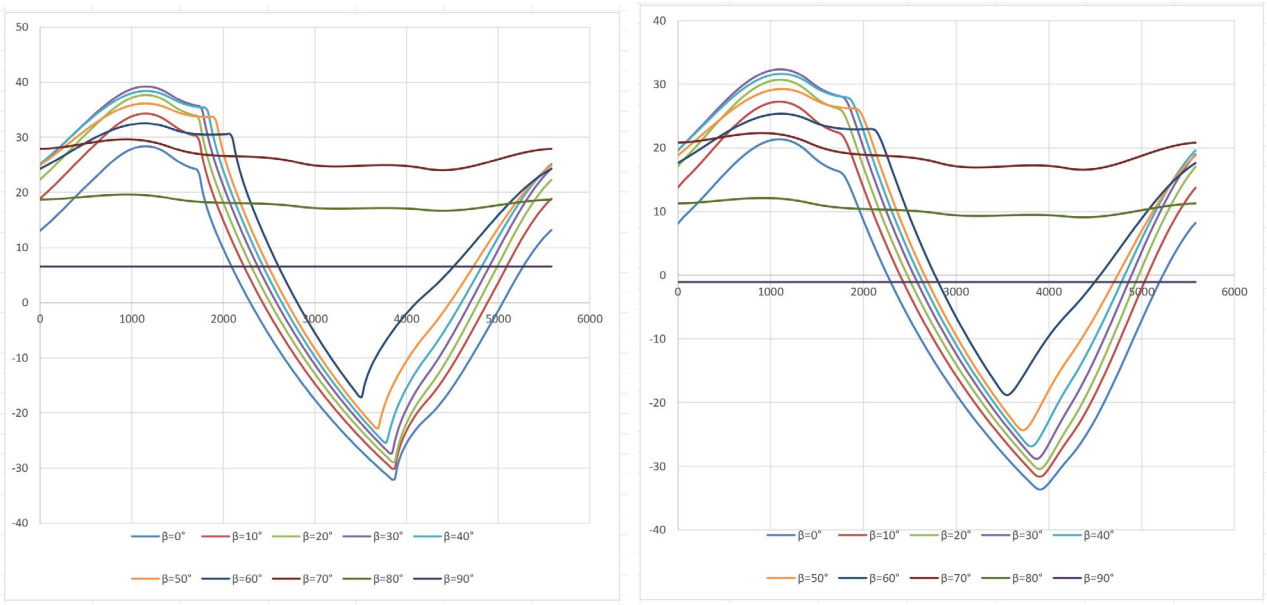

Fig. 12. Maximum(left) and minimum(right) satellite temperatures for different beta angles - orientation 1.

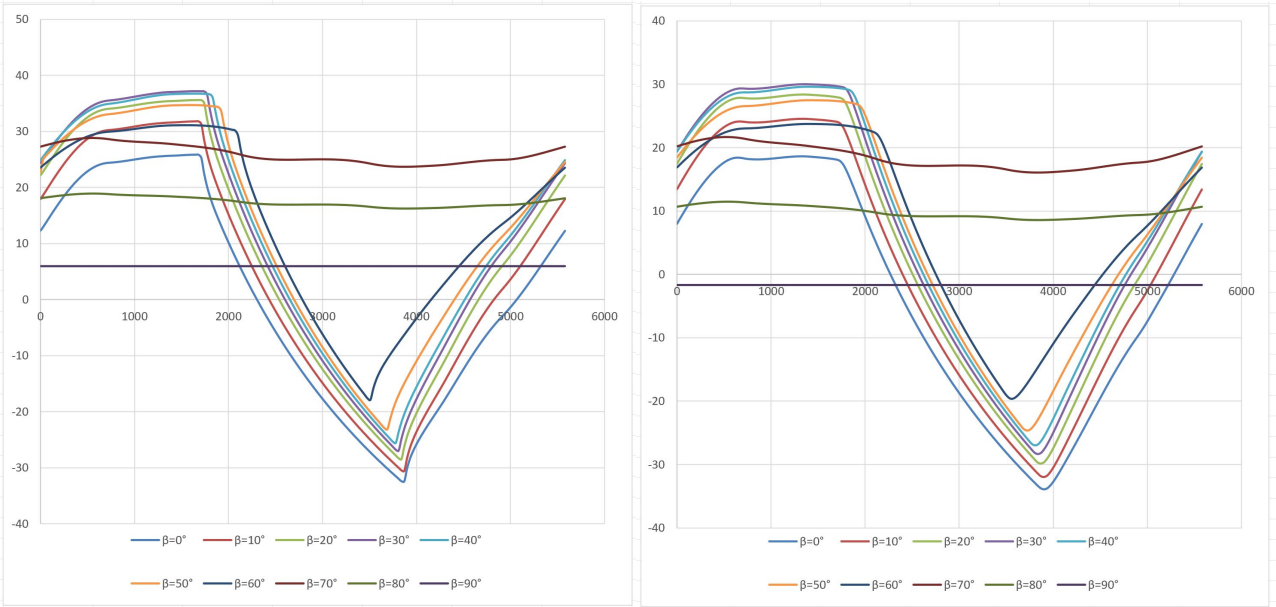

Fig. 13. Maximum(left) and minimum(right) satellite temperatures for different beta angles - orientation 2.

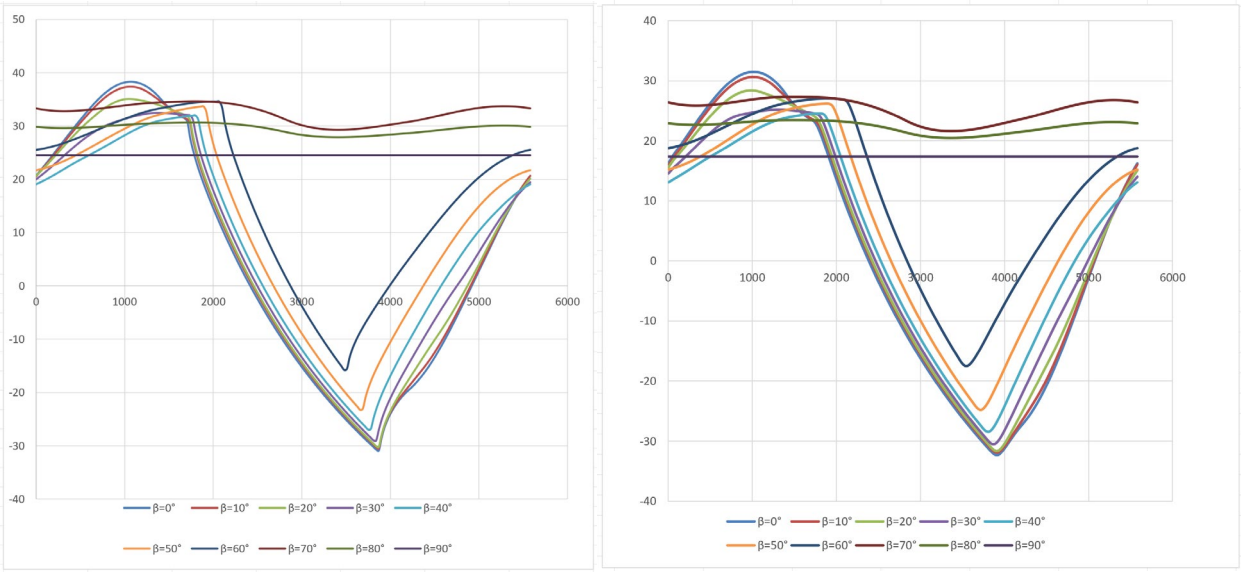

Fig. 14. Maximum(left) and minimum(right) satellite temperatures for different beta angles - orientation 3.

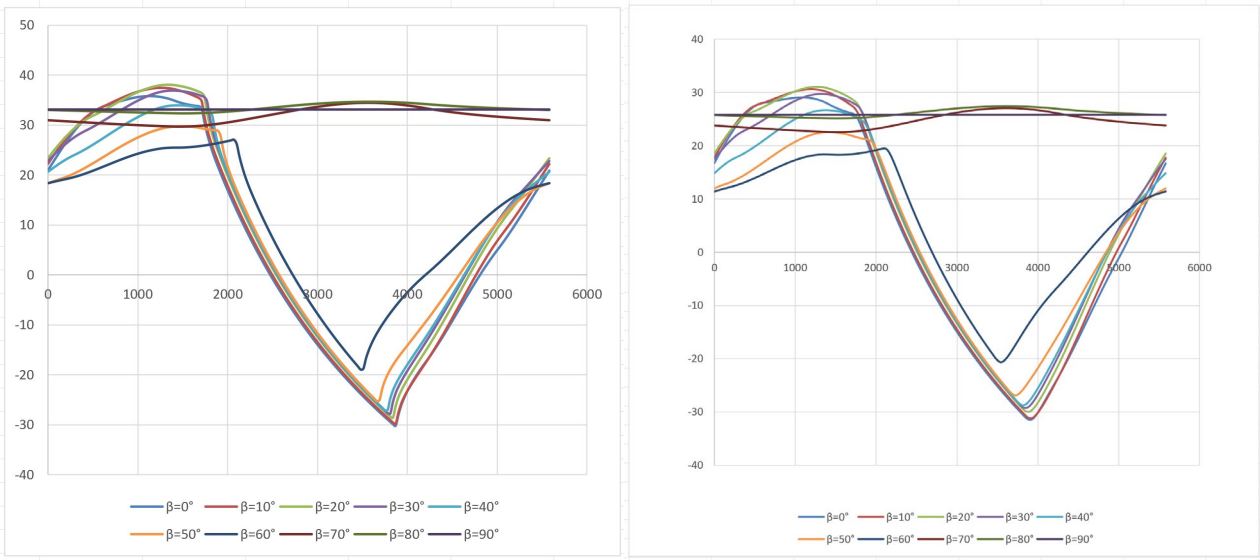

Fig. 15. Maximum(left) and minimum(right) satellite temperatures for different beta angles - orientation 4.

The segment of the graphs displaying a significant reduction in temperatures for beta angles (β) ranging from 0° to 60° corresponds to the eclipse phase. During this phase, the sole external source of heat is the infrared radiation emanating from the Earth.

At an altitude of 431 km and beta angles equal to or greater than 70°, the satellite has no eclipse period, regardless of its orientation. The graphs below show that for these beta angles (70°, 80°, 90°), the satellite did not experience large temperature oscillations since the solar irradiance and albedo were almost constant throughout the orbit.

Regarding orientations 1 and 2, maximum temperatures have occurred at beta angle 30°. At subsolar beta angles, the maximum temperature decreased because the solar radiation was incident on at most two surfaces. The minimum temperature of the satellite depended largely on the eclipse fraction. Therefore, the minimum temperatures were observed at beta angle 0°, where the eclipse period is the longest.

While for orientation 3, the extreme temperatures have occurred at beta angle 0° where the longest eclipse period happens.

Regarding orientation 4, the maximum temperature has occurred at beta 20° while the minimum at beta 0° just like the other orientations.

To summarize the information contained in the graphs, Table 4 shows the maximum temperatures for the satellite in the four orientations, with minimum temperatures highlighted in bold. Conversely, Table 5 shows the minimum temperatures for each orientation, with maximum temperatures highlighted in bold.

Table 4. Maximum satellite temperatures (°C) for different beta angle and four orientations.

	β=0°	β=10°	β=20°	β=30°	β=40°	β=50°	β=60°	β=70°	β=80°	β=90°
Orientation 1	28.391	34.301	37.674	39.217	38.411	36.143	32.528	29.623	19.629	**6.5597**
Orientation 2	25.848	31.792	35.588	37.179	36.737	34.701	31.107	28.826	18.913	**5.9636**
Orientation 3	38.294	37.378	35.067	32.448	31.972	33.688	34.591	34.625	30.645	**24.513**
Orientation 4	35.804	37.457	38.08	36.91	33.955	29.759	**27.079**	34.465	34.673	33.12

Table 5. Minimum satellite temperatures (°C) for different beta angle and four orientations.

	β=0°	β=10°	β=20°	β=30°	β=40°	β=50°	β=60°	β=70°	β=80°	β=90°
Orientation 1	-33.659	-31.651	-30.423	-28.837	-26.884	-24.358	-18.805	**16.592**	9.118	-1.0722
Orientation 2	-33.903	-31.967	-29.843	-28.342	-26.97	-24.637	-19.616	**16.066**	8.5741	-1.6742
Orientation 3	-32.312	-31.893	-31.676	-30.49	-28.44	-24.791	-17.525	**21.6**	20.458	17.354
Orientation 4	-33.903	-31.967	-29.843	-28.342	-26.97	-24.637	-19.616	**16.066**	8.5741	-1.6742

In other words, the maximum and minimum temperature profiles vary significantly across the different orientations :
In Orientations 1 and 2, maximum temperatures peak at β = 30°, reflecting the combined impact of direct solar input and residual heat.
In Orientation 3, the thermal extremes occur at β = 0°, emphasizing the influence of prolonged eclipse periods on thermal dynamics.
In Orientation 4, the highest temperatures are observed at β = 20°, driven by the specific alignment of the CubeSat with respect to the Sun and Earth.
These variations demonstrate the interplay between beta angle and orientation in determining thermal behavior. The findings stress the importance of tailoring thermal control strategies to specific mission profiles, considering both orbital parameters and satellite configurations. This intricate relationship between beta angle and orientation underscores the necessity for a nuanced approach to thermal management in CubeSats. The ability to predict and adapt to the thermal variations caused by these factors is pivotal for ensuring the reliability and efficiency of satellite operations. Consequently, it becomes imperative to design and implement tailored thermal control strategies that not only address the unique challenges posed by specific orbital parameters and configurations but also align with the overall mission objectives.
Here are some implications for CubeSat design:

- Hotspot Mitigation: The identification of thermal hotspots across various orientations underscores the need for localized thermal management solutions. Strategies such as integrating thermal spreaders, high-emissivity coatings, or phase-change materials could mitigate the risks associated with these hotspots.
- Insulation during eclipse periods: Prolonged eclipse phases at low beta angles pose cooling problems. Efficient insulation materials and passive thermal control elements are essential to maintain component functionality during these periods.
- Stabilized thermal behavior at high beta angles : Continuous solar exposure at high beta angles requires effective heat dissipation mechanisms, such as deployable heat sinks or active cooling systems.

Conclusion

This study delivers a comprehensive analysis of the thermal behavior of a 1U CubeSat, underscoring the significant impact of satellite orientation and beta angle on temperature distribution. Using finite element method simulations in COMSOL Multiphysics, it was observed that high beta angles (70° to 90°) result in prolonged solar exposure, leading to increased temperature ranges.

Conversely, lower beta angles (0° to 60°) introduce extended eclipse durations, mitigating thermal extremes. The findings suggest that mission planners should prioritize Sun-synchronous orbits with minimal beta angles and optimize satellite orientation to achieve thermal stability. These results contribute to the advancement of CubeSat thermal management strategies, promoting mission success under stringent space conditions.

Future studies could explore the integration of dynamic thermal control systems within CubeSats to address extreme temperature variations observed at high beta angles. Investigating the use of advanced materials with variable emissivity could further enhance thermal stability. Additionally, expanding simulations to include multi-unit CubeSats and varying orbital altitudes could provide more comprehensive insights into thermal behavior across different satellite configurations. Finally, coupling thermal analysis with structural and electronic component reliability studies would yield a holistic understanding of CubeSat performance in low Earth orbit.

References

[1] R.D, Karam, Satellite Thermal Control for Systems Engineer. Reston, VA: AIAA, 1998, Vol.181.

[2] Robert Siegel, John R. Howell, Thermal Radiation Heat Transfer, Hémisphère Publishing Corporation Third Edition 1992.

[3] L.A. Reyes, R. Cabriales-Gómez, C.E. Chávez, B. Bermúdez-Reyes, O. López-Botello, P. Zambrano-Robledo, Thermal modeling of CIIIASat nanosatellite: A tool for thermal barrier coating selection, Appl.Therm. Eng. 166 (2020) 114651.

[4] Murat Bulut, Nedim Sozbir, Analytical investigation of a nanosatellite panel surface temperatures for different altitudes and panel combinations, Appl. Therm. Eng. V75 (2015) 1076–1083.

[5] M. Bonnici, P. Mollicone, M. Fenech, M.A. Azzopardi, Analytical and numerical models for thermal related design of a new pico-satellite, Appl. Therm. Eng. 159 (2019) 113908.

[6] S. Corpino, M. Caldera, F. Nichele, M. Masoero, N. Viola, Thermal design and analysis of a nanosatellite in low earth orbit, Acta Astronaut. V11 (5) (2015) 247–261.

[7] Soo-Jin Kang, Oh. Hyun-Ung, On-orbit thermal design and validation of 1 U standardized CubeSat of STEP cube lab, Int. J. Aerosp. Eng. V 1–17 (2016) 2017.

[8] Róbert Kovács, Viktor Józsa, Thermal analysis of the SMOG-1 PocketQube satellite, Appl. Therm. Eng. 139 (2018) 506–513.

[9] B.A. Moffitt, J.C. Batty, Predictive thermal analysis of the combat sentinel satellite, 16th AIAA/USU Conference on Small Satellites, Logan, Utah, USA, (2002).

[10] E. Morsch Filho, V. de Paulo Nicolau, K.V. de Paiva, T.S. Possamai, A comprehensive attitude formulation with spin for numerical model of irradiance for CubeSats and Picosats, Appl. Therm. Eng. 168 (2020) 114859.

[11] Thanarasi K. Thermal analysis of cubesat in worse case hot and cold environment using FEA method. Applied Mechanics and Materials 2012; 225: 497-502.

[12] Tsai JR. Overview of satellite thermal analytical model. J of Spacecraft and Rockets 2004; 41 (1): 120-5.

[13] Reiss P. New methodologies for the thermal modelling of cubesats. 26th Annual AIAA/USU Conference on Small Satellites, Logan, Utah, USA, 2012.

[14] D.Gilmore, M. Donabedian, Spacecraft Thermal Control Handbook: Fundamental technologies, in: Spacecraft Thermal Control Handbook, Aerospace Press, 2002.

[15] J. Meseguer, I. Pérez-Grande, and A. Sanz-Andrés, Spacecraft thermal control, 1st Ed. Cambridge, UK: Woodhead Publishing, 2012.

[16] Phillipp Reiss, New methodologies for the thermal modelling of cubesats, 26th AIAA/USU Conference of Small Satellites, 2012, pp. 1–12.

[17] E. Escobar, M. Diaz, J.C. Zagal, Design automation for satellite passive thermal control, The 4S Symposium, Portoroz, Slovenia, (2012).

[18] F. Tribak, O. Bendaou and F. Nejma, Impact of orbit inclination on heat transfer in a 1 U LEO CubeSat, MATEC Web of Conferences, vol. 37, 2022.

[19] Cengel, Yunus A. Heat Transfer: A practical approach 2nd Edition. s.l. : McGraw-Hill Education , 2002.

[20] J.R. Ehlert, T.F. Smith, View factors for perpendicular and parallel rectangular plates, J. Thermophys. Heat Transfer 7 (1) (1993) 173–175.